Superconducting Transition Temperature of the Bose One-Component Plasma

Chao Zhang,[1,2] Barbara Capogrosso-Sansone,[3] Massimo Boninsegni,[4]
Nikolay V. Prokof'ev,[5] and Boris V. Svistunov[5,6]

[1]*Department of Modern Physics, University of Science and Technology of China, Hefei, Anhui 230026, China*
[2]*Hefei National Laboratory, University of Science and Technology of China, Hefei 230088, China*
[3]*Department of Physics, Clark University, Worcester, Massachusetts 01610, USA*
[4]*Department of Physics, University of Alberta, Edmonton, Alberta, Canada T6G 2H5*
[5]*Department of Physics, University of Massachusetts, Amherst, Massachusetts 01003, USA*
[6]*Wilczek Quantum Center, School of Physics and Astronomy, Shanghai Jiao Tong University, Shanghai 200240, China*

We present results of numerically exact simulations of the Bose one-component plasma, i.e., a Bose gas with pairwise Coulomb interactions among particles and a uniform neutralizing background. We compute the superconducting transition temperature for a wide range of densities, in two and three dimensions, for both continuous and lattice versions of the model. The Coulomb potential causes the weakly interacting limit to be approached at high density, but gives rise to no qualitatively different behavior, *vis-à-vis* the superfluid transition, with respect to short-ranged interactions. Our results are of direct relevance to quantitative studies of bipolaron mechanisms of (high-temperature) superconductivity.

Introduction.—Reliably estimating the critical temperature (T_c) for the superconducting transition in a correlated Fermi system—even with relatively large uncertainties—is a difficult task. Exponential sensitivity of T_c to system parameters leads to the challenge of accurate and unbiased treatment of many-body correlation effects. An exception to this rule is dimerized states when pairing of fermions takes place in real, rather than momentum, space, and the system can be effectively regarded as an assembly of interacting Bose particles.

Remarkably, the value of T_c in the three-dimensional (3D) interacting Bose system is very close to the Bose-Einstein condensation point for the ideal gas, $T_c^{(0)} \approx 3.31(n^{2/3}/m)$, where n is the number density and m the particle mass (we use units in which $\hbar = k_B = 1$), when interactions are short range. This holds all the way (within, say, a factor of 2) from the dilute gas limit to interparticle distances of the order of the potential range; for the case of superfluid ^{4}He, for example, it is $T_c/T_c^{(0)} \approx 0.7$. The archetypal model displaying this physical behavior is a Bose fluid of particles interacting via short-ranged, hard-core potentials [1–4].

In two dimensions (2D) there is no Bose-Einstein condensation, but in the presence of interactions a Bose fluid undergoes a Berezinskii-Kosterlitz-Thouless (BKT) superfluid transition, which is theoretically well understood and, for a gas with short-ranged interactions, precisely characterized quantitatively [5]. In a broad range of density (including the regime of strong correlations [3]), it is $T_c \approx 1.3T^{(0)}$ with $T^{(0)} = (n/m)$. Thus, an approximate estimate for T_c is given by

$$T_c \approx C_d \frac{n^{2/d}}{m}, \quad \text{with} \quad C_d = \begin{cases} 1.30, & d = 2 \\ 3.31, & d = 3 \end{cases} \quad (1)$$

d being the dimensionality. Equation (1) can also be utilized to estimate T_c for a system of dimerized fermions with short-ranged interactions, upon replacing m with the effective dimer mass $m^\star$.

Recently, interest in dimerized Fermi systems has been renewed by proposals of bipolaron (high-temperature) superconductivity [6–11]. It was found that bipolarons emerging in lattice models with phonon-modulated hopping feature relatively light effective masses and small size, making them potential candidates for a new class of high-temperature superconductors [11]. At large distances bipolarons interact via the long-range electrostatic (Coulomb) potential. So far, this aspect of the problem has not been addressed quantitatively, as only models with short-range repulsion have been studied.

The long-range character of interactions leads to a number of fundamental questions and changes, including the reversal of the relation between the low-density and weak-interaction limits. In a Coulomb system, the dimensionless coupling parameter—the Wigner-Seitz radius r_s—is defined as follows in 2D and 3D:

$$r_s = \frac{1}{a_B n^{1/d}} \times \begin{cases} \pi^{-1/2}, & d = 2, \\ (4\pi/3)^{-1/3}, & d = 3, \end{cases} \quad (2)$$

a_B being the Bohr radius. The perturbative regime ($r_s \ll 1$) now corresponds to the limit of high density, where the very

notion of compact bipolarons may become ill defined, while in the low-density limit ($r_s \gg 1$) strong correlations may result in large deviations of T_c from the ideal gas value.

On the one hand, this raises the question of the applicability of Eq. (1) to realistic bipolaronic systems, calling for a reliable, quantitative verification based on unbiased, robust theoretical methods; on the other hand, the prospects of bipolaron superconductivity with large T_c contribute to the fundamental interest in the superconductivity of a charged Bose gas and its broad relevance in astrophysics [12,13].

A system of charged particles in the presence of a neutralizing, uniform charge background is typically referred to as the one-component plasma (OCP). It has been extensively investigated in the classical case [14–18], and there exists also a number of studies of its quantum phase diagram, for both types of quantum statistics [19–28]. However, to the best of our knowledge a systematic study of the superconducting transition for the boson case, especially in the interesting $r_s \gtrsim 1$ regime, is still missing.

In this Letter, we determine the superconducting transition critical temperature (as a function of r_s) in the Bose OCP, in 2D and 3D, using state-of-the-art computer simulations. Besides the continuous-space system, we consider a lattice model in order to gauge the effects of long-range interactions against discreteness of space and/or extra short-ranged repulsion. Our results are numerically "exact," i.e., statistical and systematic errors can be rendered negligible in practice, using ordinary computing infrastructure. We use the lattice [29] and continuous-space [30] versions of the worm algorithm.

In order to account for the long-range character of the Coulomb interaction, we used the Ewald summation method in the pairwise form (see, for instance, Refs. [31,32]) in our lattice simulations; for simulations in continuous space we made use of the modified periodic Coulomb scheme of Fraser et al. [33], affording greater computational efficiency. Both schemes are exact, when extrapolated to the infinite-size limit.

Our key results are presented in Figs. 1 and 2. We use $T_c^{(0)}$ ($T^{(0)}$), defined in the Introduction, as our reference temperature in 3D (2D). In 3D, we find the effect of Coulomb interactions to be surprisingly weak. At $r_s < 10$, the difference between T_c and $T_c^{(0)}$ is within ~1%, remaining less than 5% up to $r_s = 25$. The effects of discreteness and on site repulsion—rather small on the absolute scale—are more important than the effects of Coulomb forces.
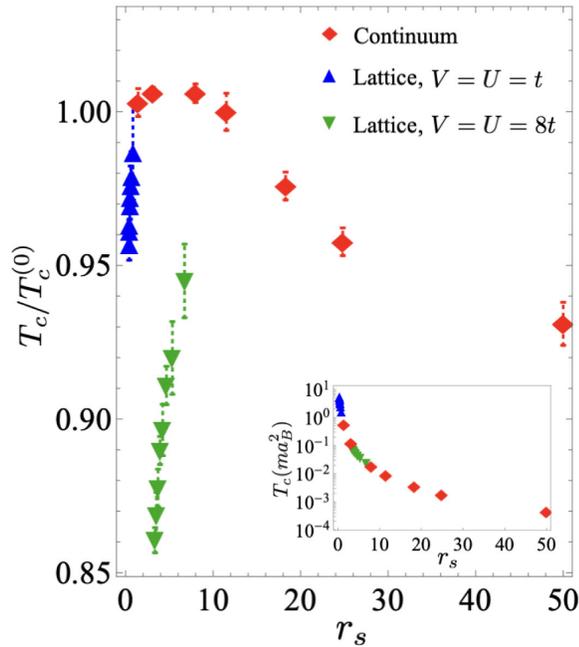

FIG. 1. Transition temperature (in units of $T_c^{(0)}$) in 3D as a function of r_s; see Eq. (2). Blue up and green down triangles correspond to the lattice models with $V = U = t$ and $V = U = 8t$, respectively. Red diamonds correspond to the continuous-space model. If not visible, error bars are within symbol size. Note that different values of V/t correspond to different values of the Bohr radius a_B on a lattice (see text), and this must be taken into account when comparing lattice and continuum results for the same r_s. Inset: T_c [in the unit of $1/(ma_B^2)$] as a function of r_s.
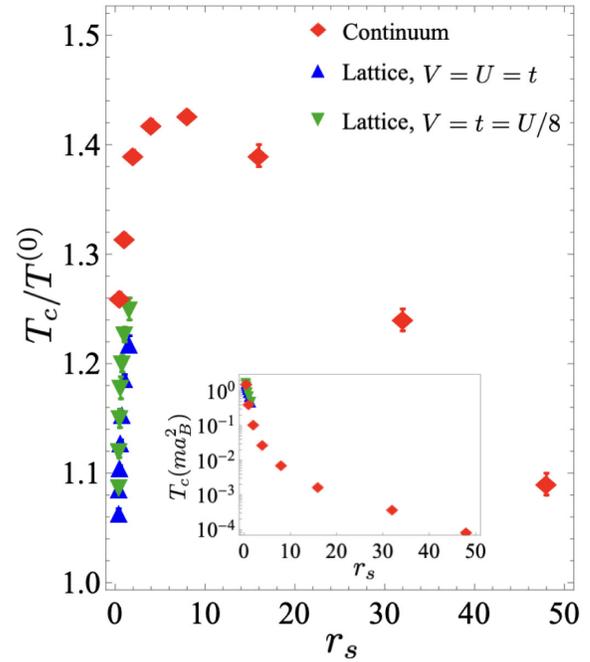

FIG. 2. Transition temperature (in units of $T^{(0)}$) in 2D as a function of r_s. Blue up and green down triangles correspond to the lattice models with $V = U = t$ and $V = t = U/8$, respectively. Red diamonds correspond to the continuous-space model. Inset: T_c [in the unit of $1/(ma_B^2)$] as a function of r_s. If not visible, error bars are within symbol size.

The situation in 2D is similar. Here the critical temperature reaches its maximum value $T_c^{(\max)} \approx 1.43 T^{(0)}$ at $r_s \approx 8$ and then slowly decreases with increasing r_s, in a qualitative analogy with the 3D case, but with somewhat more pronounced quantitative effect of about 30%. We traced the dependence of T_c on r_s up to $r_s = 48$, beyond which the superconducting, Wigner crystal, hexatic, normal metal, and emulsion phases [34] start competing with each other [27,28]. As one might have expected by analogy with the known behavior of the weakly interacting 2D Bose gas with short-range interaction, the small-r_s regime is characterized by a moderate suppression of T_c compared with $T_c^{(\max)}$. Thus, the estimate [Eq. (1)] remains rather accurate in both 3D and 2D.

The models.—The continuous-space OCP model is standard (see, for instance, Ref. [27]). The lattice version is described by the following Hamiltonian on the hypercubic lattice, with periodic boundary conditions (to ensure uniform density):

$$\hat{H} = -t \sum_{\langle \mathbf{i},\mathbf{j} \rangle} (\hat{a}_{\mathbf{i}}^{\dagger} \hat{a}_{\mathbf{j}} + \text{H.c.}) + \frac{U}{2} \sum_{\mathbf{i}} \hat{n}_{\mathbf{i}}^2 + \frac{V}{2} \sum_{\mathbf{i} \neq \mathbf{j}} \frac{\hat{n}_{\mathbf{i}} \hat{n}_{\mathbf{j}}}{|\mathbf{i}-\mathbf{j}|}. \quad (3)$$

Here, the $\langle \mathbf{i}, \mathbf{j} \rangle$ sum runs over all pairs of nearest-neighbor sites indexed by integer vectors, $\hat{a}_{\mathbf{i}}$ and $\hat{n}_{\mathbf{i}} = \hat{a}_{\mathbf{i}}^{\dagger} \hat{a}_{\mathbf{i}}$ are the Bose annihilation operator and occupation number on site $\mathbf{i}$, respectively; t is the hopping amplitude, U is the on site (Hubbard) repulsion, and V is the amplitude of the repulsive Coulomb potential.

In the model [Eq. (3)], the essential—up to the choice of units—dependence of T_c is three-parametric. A natural set of three dimensionless parameters consists of U/t, V/t, and the filling factor $n = \langle n_{\mathbf{i}} \rangle$. In this Letter, we are not interested in the effects of commensurability (e.g., Mott physics), which model (3) definitely demonstrates at $n = 1, 1/2$, and other commensurate fillings (at strong enough interactions); hence, we work with $n \leq 0.4$.

In the $n \to 0$ limit, Eq. (3) reproduces the single-parametric continuous-space behavior because U/t becomes irrelevant, and V/t and n are absorbed into a single parameter r_s. The expression for r_s in terms of V/t and n readily follows from Eq. (2) by relating density and filling factor by a^d and noting that for the tight-binding dispersion relation $m = 1/2a^2 t$. Then, the amplitude of the Coulomb potential at the lattice spacing, $V = e^2/a$, immediately leads to $a_B = 1/(mVa) = a(2t/V)$ (for large V/t we formally have $a_B/a \ll 1$ implying that lattice effects are more pronounced at large r_s).

One question, of both fundamental and applied (see the numeric protocol below) interest, is whether the long-range Coulomb interaction changes the universality class of the superfluid transition [35]. It is easy to argue (and validate numerically) that the transition remains in the d-dimensional XY universality class observed in systems with short-range interactions. Indeed, the qualitative effect of the long-range potential—incompressibility of the system—does not change properties of large-scale vortexes, which are the degrees of freedom responsible for the XY criticality (see, e.g., Ref. [36]). Along similar lines, recall that the classical XY model itself is "incompressible" by construction because it lacks degrees of freedom associated with density.

Numerical protocols.—We simulate our models with the lattice [29] and continuous-space [30] versions of the worm algorithm. The key observable is the mean-square world-line winding number, $\langle W^2 \rangle = \sum_{i=1}^{d} \langle W_i^2 \rangle / d$, where W_i is the winding number of the particle paths along the i direction. In the thermodynamic limit $L \to \infty$ (L is the linear size of the hypercubic simulation cell), this quantity gives access to the superfluid stiffness, Λ_s, via the Pollock-Ceperley formula [37]:

$$\Lambda_s = \frac{\langle W^2 \rangle T}{L^{d-2}} \qquad (L \to \infty). \quad (4)$$

In the 3D case, thanks to scale invariance of the 3D XY criticality, it is more convenient to work directly with $\langle W^2 \rangle$. At T_c, this quantity saturates to the universal (system- and L-independent) constant 0.516(1) [38], while at $T < T_c$ ($T > T_c$) it diverges (vanishes) as $L \to \infty$. These properties lead to simple and accurate schemes (illustrated in Figs. 3 and 4) of extracting T_c and automatically validating that the
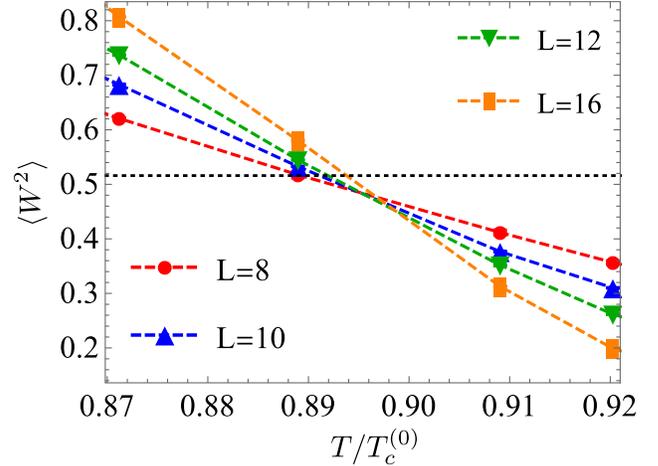

FIG. 3. Determining critical temperature of the 3D model [Eq. (3)] from the crossing point of the mean-square winding number curves, $\langle W^2 \rangle$, computed for system sizes $L = 8, 10, 12$, and 16 (red circles, blue squares, green up triangles, and orange down triangles, respectively) as functions of temperature. In this example, $U = V = 8t$ and $n = 0.2$ (corresponding to $r_s = 4.24$). If not visible, error bars are within symbol size. The crossing points' locations pinpoint $T_c = 0.896(5) T_c^{(0)}$, and their vertical values are close to the 3D XY universality prediction of 0.516(1) [38] shown with a horizontal dashed line; small deviations from 0.516 are explained by leading corrections to scaling (see the text and Fig. 4).
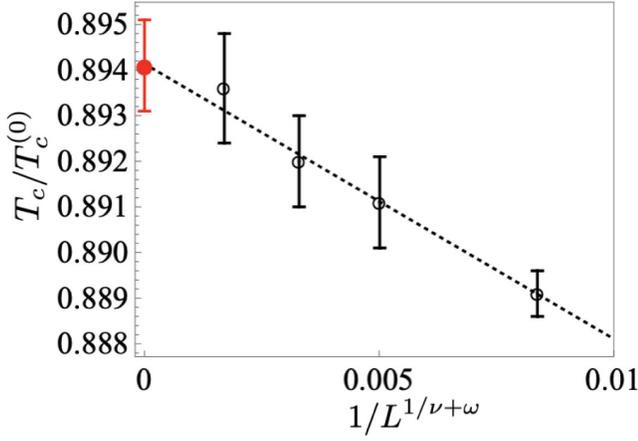
FIG. 4. Extracting T_c from the known behavior of the leading correction to scaling at the 3D XY criticality (see the text). The system's parameters are the same as in Fig. 3. The extrapolated critical temperature is estimated as $T_c = 0.8941(10)T_c^{(0)}$ (red dot).
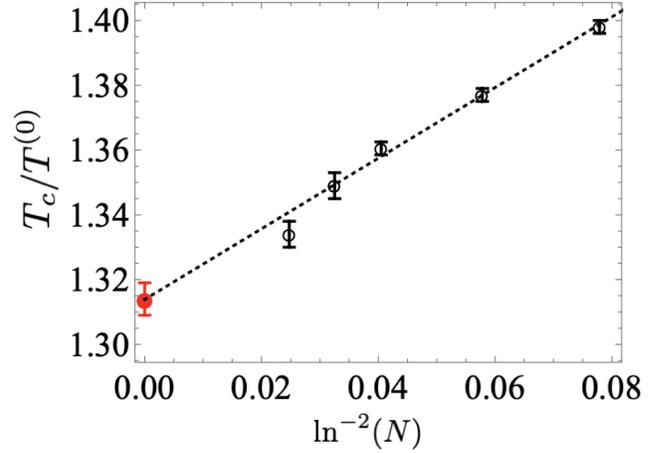

FIG. 5. Finite-size scaling of the "critical" temperature $T_c(N)$ for the 2D continuous system at $r_s = 1.0$. The simulations were performed in a square cell with $N = 36$, 64, 144, 256, and 576 particles. After extrapolation to the $N \to \infty$ limit we obtain $T_c = 1.314(5)T^{(0)}$ (red dot).

universal 3D XY critical behavior does take place (from the dependence of $\langle W^2 \rangle$ on T at different L's). System sizes $L \le 16$ prove sufficient for obtaining results for T_c in the model [Eq. (3)] with subpercent accuracy.

As expected, the values of $\langle W^2 \rangle$ at the crossing points in Fig. 3 are close to the universal 3D XY number. They are supposed to deviate from 0.516 due to corrections to scaling, with the leading term vanishing as $1/L^\omega$ with $\omega \approx 0.8$ [38]. Taking this correction into account and obtaining a more accurate scheme for determining T_c are achieved in two simple steps. First, define the "finite-size" critical temperature $T_c(L)$ by the condition $\langle W^2 \rangle = 0.516(1)$. Second, utilize the fact that the finite-size correction $\Delta T_c = T_c(L) - T_c(\infty)$ vanishes as $1/L^{1/\nu+\omega}$, with $\nu = 0.6717$ being the 3D XY correlation length exponent [38], to extrapolate $T_c(L)$ to the thermodynamic limit. This scheme is illustrated in Fig. 4. Note that the straight-line behavior of ΔT_c as a function of $1/L^{1/\nu+\omega}$ is yet another validation of the 3D XY criticality.

The 2D case is different because the BKT transition lacks scale invariance. However, its asymptotically exact critical theory [39–41] allows one to eliminate the leading finite-size correction and obtain accurate thermodynamic limit results. Specifically, for a given number of particles, N, we define the "critical" temperature $T_c(N)$ as the temperature at which the ratio $\Lambda_s/T = \langle W^2 \rangle$ equals to its universal Nelson-Kosterlitz value of $2/\pi$ [41,42], in complete analogy with the 3D case discussed above. Kosterlitz-Thouless renormalization-group theory predicts that the leading finite-size correction to $\Delta T_c = T_c(N) - T_c(\infty)$ scales as $1/\ln^2 N$. This law is used to extrapolate $T_c(N)$ to the $N \to \infty$ limit, and automatically validate the applicability of the BKT theory by the observation of this (very specific)

finite-size effect. The corresponding protocol is illustrated in Fig. 5.

Figures 1 and 2 show final results for T_c, in 3D and 2D, respectively, as a function of r_s defined by Eq. (2). In 2D, on approaching the Wigner crystal phase, which is estimated to emerge first at $r_s > 50$, the phase diagram is determined by competition between the Wigner crystal, hexatic, superconductor, normal liquid, and an infinite set of emulsion phases [28,34]. Studies of this parameter regime go well beyond the scope of this Letter. In 3D, we restricted our study to $r_s \le 50$, which corresponds to densities all the way down to $na_B^3 \sim 10^{-5}$ (for greater values of r_s, we start observing finite-T Wigner crystal states in accessible simulation cells).

Conclusions.—Motivated by recent progress with quantifying scenarios of high-temperature bipolaron superconductivity, we studied the effect of Coulomb interactions on the critical temperature of the superconducting transition in the 2D and 3D Bose OCP, both on a lattice and in continuous space. We provide evidence that the superconducting transition is in the XY universality class and obtain values for the critical temperature T_c in a broad range of densities.

Screening of long-range interactions works in the direction of reducing their effect on T_c. However, screening of $q \to 0$ modes involves divergent timescales (this is the prime reason for having plasmons instead of sound waves) making our finding that T_c shifts are remarkably modest all the way to the Wigner crystal phase, surprising. The estimate [Eq. (1)] remains quantitatively accurate and similar to that for systems with short-range interactions—up to the reversal of the small and large density limits controlling the strength of interaction-induced correlations. The role of

interactions is twofold: (i) On one hand (this aspect is conceptually important and well pronounced in 2D), interactions suppress thermal fluctuations of the superfluid order parameter amplitude (but not the phase), thereby contributing to the increase of T_c; (ii) on the other hand, strong local correlations caused by interactions increase phase fluctuations and suppress T_c. In a Coulomb system, the first effect is dominant at $r_s < 5$ (high-density limit) while the second effect takes over at $r_s > 10$ (low-density regime). The result of this competition is the $T_c/T_c^{(0)}$ vs r_s curve with a maximum at $r_s \sim 8$; see Figs. 1 and 2.

We expect that our precise data for the dependence of T_c on r_s will prove important in the context of experimental realization of a relatively dilute, and, thus, well-defined bipolaron superconductor.

[1] P. Grüter, D. Ceperley, and F. Laloë, Phys. Rev. Lett. **79**, 3549 (1997).

[2] K. Nho and D. P. Landau, Phys. Rev. A **70**, 053614 (2004).

[3] S. Pilati, S. Giorgini, and N. Prokof'ev, Phys. Rev. Lett. **100**, 140405 (2008).

[4] Y. Kora, M. Boninsegni, D. T. Son, and S. Zhang, Proc. Natl. Acad. Sci. U.S.A. **117**, 27231 (2020).

[5] N. Prokof'ev, O. Ruebenacker, and B. Svistunov, Phys. Rev. Lett. **87**, 270402 (2001).

[6] D. J. J. Marchand, G. De Filippis, V. Cataudella, M. Berciu, N. Nagaosa, N. V. Prokof'ev, A. S. Mishchenko, and P. C. E. Stamp, Phys. Rev. Lett. **105**, 266605 (2010).

[7] J. Sous, M. Chakraborty, R. V. Krems, and M. Berciu, Phys. Rev. Lett. **121**, 247001 (2018).

[8] C. Zhang, N. V. Prokof'ev, and B. V. Svistunov, Phys. Rev. B **104**, 035143 (2021).

[9] M. R. Carbone, A. J. Millis, D. R. Reichman, and J. Sous, Phys. Rev. B **104**, L140307 (2021).

[10] C. Zhang, N. V. Prokof'ev, and B. V. Svistunov, Phys. Rev. B **105**, L020501 (2022).

[11] C. Zhang, J. Sous, D. R. Reichman, M. Berciu, A. J. Millis, N. V. Prokof'ev, and B. V. Svistunov, Phys. Rev. X **13**, 011010 (2023).

[12] B. W. Ninham, Phys. Lett. A **4**, 278 (1963).

[13] V. L. Ginzberg, Astrophys. Space Phys. Rev. **1**, 81 (1969).

[14] E. E. Salpeter, Ann. Phys. (N.Y.) **5**, 183 (1958).

[15] R. Abe, Prog. Theor. Phys. **22**, 213 (1959).

[16] S. G. Brush, J. Chem. Phys. **45**, 2102 (1966).

[17] W. L. Slattery, G. D. Doolen, and H. E. DeWitt, Phys. Rev. A **21**, 2087 (1980).

[18] M. Baus and J. P. Hansen, Phys. Rep. **59**, 1 (1980).

[19] A. L. Fetter, Ann. Phys. (N.Y.) **64**, 1 (1971).

[20] S.-K. Ma, Phys. Rev. Lett. **29**, 1311 (1972).

[21] P. V. Panat, H. E. DeWitt, and J. C. Garrison, Phys. Lett. **43A**, 130 (1973).

[22] R. F. Bishop, J. Low Temp. Phys. **15**, 601 (1974).

[23] D. M. Ceperley and B. J. Alder, Phys. Rev. Lett. **45**, 566 (1980).

[24] G. Ortiz and P. Ballone, Phys. Rev. B **50**, 1391 (1994).

[25] S. Moroni, D. M. Ceperley, and G. Senatore, Phys. Rev. Lett. **75**, 689 (1995).

[26] M. D. Jones and D. M. Ceperley, Phys. Rev. Lett. **76**, 4572 (1996).

[27] S. De Palo, S. Conti, and S. Moroni, Phys. Rev. B **69**, 035109 (2004).

[28] B. K. Clark, M. Casula, and D. M. Ceperley, Phys. Rev. Lett. **103**, 055701 (2009).

[29] N. V. Prokof'ev, B. V. Svistunov, and I. S. Tupitsyn, Zh. Eksp. Teor. Fiz. **114**, 570 (1998) [J. Exp. Theor. Phys. **87**, 310 (1998)].

[30] M. Boninsegni, N. V. Prokof'ev, and B. V. Svistunov, Phys. Rev. E **74**, 036701 (2006).

[31] S. Yi, C. Pan, and Z. Hu, J. Chem. Phys. **147**, 126101 (2017).

[32] D. Wang, J. Liu, J. Zhang, S. Raza, X. Chen, and C.-L. Jia, Comput. Mater. Sci. **162**, 314 (2019).

[33] L. M. Fraser, W. M. C. Foulkes, G. Rajagopal, R. J. Needs, S. D. Kenny, and A. J. Williamson, Phys. Rev. B **53**, 1814 (1996), specifically Eq. (68).

[34] B. Spivak and S. A. Kivelson, Phys. Rev. B **70**, 155114 (2004).

[35] Equation (3) does not include coupling to the dynamic vector potential field. For the purpose of estimating T_c in realistic systems with percent accuracy this weak relativistic effect is not relevant. It does change the universality class of the superconducting transition: In 3D, it converts the XY universality class into inverted XY; in 2D, it turns the BKT transition into a crossover (see, e.g., Ref. [36]). These changes develop only in the close vicinity of T_c when superconducting correlations are already set over large distances, and, thus, may not affect T_c results derived on the basis of Eq. (3).

[36] B. Svistunov, E. Babaev, and N. Prokof'ev, *Superfluid States of Matter* (Taylor & Francis, London, 2015).

[37] E. L. Pollock and D. M. Ceperley, Phys. Rev. B **36**, 8343 (1987).

[38] M.-C. Cha, M. P. A. Fisher, S. M. Girvin, M. Wallin, and A. P. Young, Phys. Rev. B **44**, 6883 (1991); M. Campostrini, M. Hasenbusch, A. Pelissetto, P. Rossi, and E. Vicari, Phys. Rev. B **63**, 214503 (2001); E. Burovski, J. Machta, N. Prokof'v, and B. Svistunov, Phys. Rev. B **74**, 132502 (2006); M. Campostrini, M. Hasenbusch, A. Pelissetto, and E. Vicari, Phys. Rev. B **74**, 144506 (2006).

[39] J. M. Kosterlitz and D. J. Thouless, J. Phys. C **5**, L124 (1972); **6**, 1181 (1973).

[40] J. M. Kosterlitz, J. Phys. C **7**, 1046 (1974).

[41] D. R. Nelson and J. M. Kosterlitz, Phys. Rev. Lett. **39**, 1201 (1977).

[42] Strictly speaking, the exact critical relation in terms of $\langle W^2 \rangle$ is geometry dependent and for the square system should be corrected as $\langle W^2 \rangle \approx 2/\pi - 32e^{-4\pi}$, see Ref. [43]. However, the difference with $2/\pi$ is at the level of the fourth significant digit—orders of magnitude smaller than statistical error bars on $\langle W^2 \rangle$.

[43] N. V. Prokof'ev and B. V. Svistunov, Phys. Rev. B **61,** 11282 (2000).